Negative Thermal Expansion in $(Hf,Ti)Fe_2$ Induced by the Ferromagnetic and Antiferromagnetic Phase Coexistence

Yongqiang Qiao,[†] Yuzhu Song,[†] Kun Lin,[†] Xinzhi Liu,[‡] Alexandra Franz,[‡] Yang Ren,[§] Jinxia Deng,[†] Rongjin Huang,[⊥] Laifeng Li,[⊥] Jun Chen,[*,†] and Xianran Xing[†]

[†]Beijing Advanced Innovation Center for Materials Genome Engineering, and Department of Physical Chemistry, University of Science and Technology Beijing, Beijing 100083, China

[‡]Helmholtz-Zentrum Berlin für Materialien und Energie, 14109 Berlin, Germany

[§]X-Ray Science Division, Argonne National Laboratory, Argonne, Illinois 60439, United States

[⊥]Key Laboratory of Cryogenics, Technical Institute of Physics and Chemistry, Chinese Academy of Sciences, Beijing, China.

Supporting Information Placeholder

ABSTRACT: Negative thermal expansion (NTE) is an intriguing physical phenomenon, which can be used to the applications of thermal expansion adjustment of materials. In this study, we report a NTE compound of $(Hf,Ti)Fe_2$, while both end members of $HfFe_2$ and $TiFe_2$ show positive thermal expansion. The results reveal that phase coexistence is detected in the whole NTE zone, in which one phase is ferromagnetic (FM), while the other is antiferromagnetic (AFM). With increasing temperature, the FM phase is gradually transformed to the AFM one. The NTE phenomenon occurs in the present $(Hf,Ti)Fe_2$ due to the fact that unit cell volume of the AFM phase is smaller than that of the FM phase, and the mass fraction of the AFM phase increases with increasing temperature. The construction of phase coexistence can be a method to achieve NTE materials in future studies.

KEYWORDS: negative thermal expansion, magnetic phase coexistence, intermetallic compounds

Most materials expand upon heating due to the anharmonic vibration of adjacent atoms, which show positive thermal expansion (PTE). PTE materials are widely used in industrial applications, but inevitably leading to device failure because of the mismatch of coefficients of thermal expansion (CTE). At this point, it is particularly important to explore negative thermal expansion (NTE) or zero thermal expansion (ZTE) materials. Up to now, the great achievements have been made in this field, such as oxides,[1-3] alloys,[4-9] Mn-based antiperovskites,[10-12] fluorides,[13-18] $PbTiO_3$-based ferroelectrics,[19-21] and cyanides.[22,23]

In the process of exploring NTE materials, various mechanisms were used to explain the NTE phenomena, such as rigid unit modes,[24] spontaneous volume ferroelectrostriction,[25,26] magneto-volume effect,[4-9] size effect,[27,28] electronic valence transition,[29,30] and "guitar-string" effect.[16] In addition to these mechanisms mentioned above, phase coexistence is also an effective method. A good example is $Bi_{0.95}La_{0.05}NiO_3$,[29] in which the phase coexistence is observed between 300 and 370 K. A linear fit to the weighted average volumes behaves intriguing NTE, since the volume of low-temperature triclinic phase is larger than that of high-temperature orthorhombic one. The phase coexistence could be possible method to find new NTE materials. It has been known that unit cell volume of ferromagnetic (FM) structure is usually larger than that of antiferromagnetic (AFM) ones.[4,31,32] If the above two magnetic structures can coexist in a magnetic material, NTE could be discovered.

In this paper, we report a NTE induced by magnetic phase coexistence in $(Hf,Ti)Fe_2$-based compounds. The present material shows a wide NTE temperature range including room temperature. Furthermore, ZTE can be achieved by adjusting the concentration of Ti. The NTE property has been studied by the synchrotron X-ray diffraction (SXRD), neutron powder diffraction (NPD), and macroscopic magnetic measurements, which reveals the relationship between NTE and magnetic phase coexistence. The understanding on this relationship will be helpful for the research on other NTE materials in future.

The temperature dependence of the SXRD data of $Hf_{0.6}Ti_{0.4}Fe_2$ was analyzed by the Rietveld method. The SXRD patterns above 345 K can be well fitted using the structure with the space group of $P6_3/mmc$ (Figure S1). However, the diffraction peaks begin to split below 345 K (Figure 1a). To highlight this feature clearly, the (302) peak is analyzed separately (Figure 1b). It can be clearly seen that the single peak becomes to split into two ones as temperature is below 345 K. In order to depict the split peaks in the following discussions, the left peak is defined as H1, the right one as H2, and the single one at high temperatures as H3. The temperature dependence of the intensity of the H2 peak is indicated by the red arrow (Figure 1b), and the relative intensity of this peak increases upon heating. In addition, the profiles of H3 at high temperatures show an asymmetry character which may be due to the compositional inhomogeneity at nanoscale, even though no pronounced compositional inhomogeneity can be found by the analyses of energy dispersive spectroscopy (Figure S4).

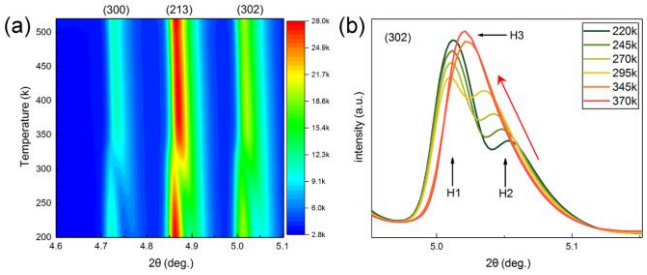

Figure 1. Temperature dependence of (a) contour plots of the (300), (213) and (302) SXRD profile intensity, and (b) the (302) diffraction peak.

To make clear structure information of the split peaks, it was carefully contrasted that the difference of SXRD patterns below and above 345 K. Interestingly, all split peaks are accompanied by the original ones just like H1 and H2, and no extra peaks can be detected. This indicates that those patterns below 345 K can be refined by two phases with the same crystal structure. Considering that the SXRD patterns above 345 K can be well refined with the space group $P6_3/mmc$, the two-phase model with the same space group $P6_3/mmc$ was used for the refinements of the split patterns. As a result, a good fitting with the two-phase model can be observed (Figure 2), in which the inset is the enlarged region showing an apparent split character. It is interesting to find that the two phases share the same space group, but with a slight difference in lattice parameter. The phenomenon of the two-phase coexistence with the same space group can be also found in the NTE Mn_3ZnN.[33]

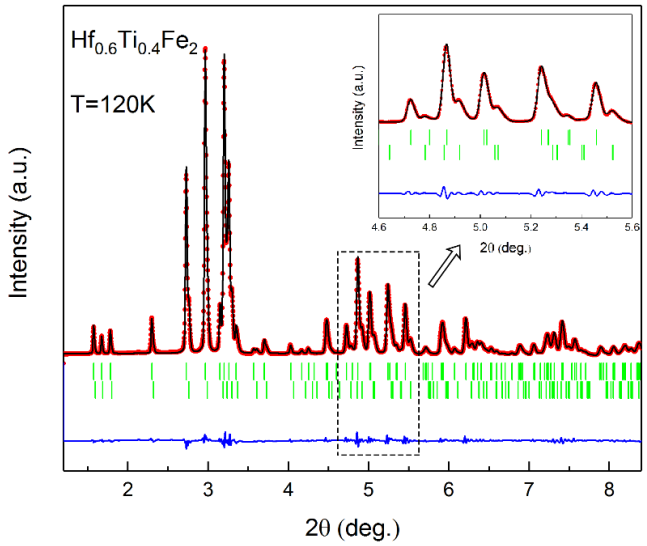

Figure 2. The full-profile refinement of the SXRD pattern of $Hf_{0.6}Ti_{0.4}Fe_2$ at 120 K by the two-phase model. The inset shows the enlarged region which has an apparent splitting character.

After the structural refinements (the two-phase model for 120 ~ 295 K; the single-phase model for 345 ~ 525 K), temperature dependence of unit cell volume of $Hf_{0.6}Ti_{0.4}Fe_2$ is plotted in Figure 3a. It can be seen that unit cell volumes of all phases increase with increasing temperature. In the temperature range from 120 K to 295 K, the unit cell volume of H1 phase is larger than that of H2. Above the temperature of 345 K, the phenomenon of phase separation disappears and the unit cell volume displays a normal thermal expansion character. Most interestingly, although the unit cell volumes of the H1 and H2 phases all expand upon heating, the macroscopic linear thermal expansion decreases with increasing temperature (Figure 3c). The linear CTE of $Hf_{0.6}Ti_{0.4}Fe_2$ is $\alpha_l = -2.2 \times 10^{-6}\ K^{-1}$ (120 ~ 325 K, ΔT = 205 K). To reveal this novel NTE phenomenon, temperature dependence of the mass fractions of two phases of H1 and H2 were extracted from the structural refinements (Figure 3b). With increasing temperature, the mass fraction of the H1 phase decreases gradually before reaching 345 K, while the H2 phase shows an opposite behavior. To get the average unit cell volume in the temperature range of phase coexistence, the law of mixtures is used by the following formula: $V_{average} = V_{H1} \times \omega_{H1} + V_{H2} \times \omega_{H2}$, where $V_{average}$ stands for the average unit cell volume, while V_{H1} and V_{H2} represent the unit cell volumes of the H1 and H2 phases, respectively. ω_{H1} and ω_{H2} are on behalf of the mass fraction of correlative phases. When the relevant parameters are put into this formula, it is interesting to find that the average unit cell volume exhibits NTE in the temperature range from 120 K to 295 K (Figure 3c). The corresponding CTE value is $\alpha_V = -4.2 \times 10^{-6}\ K^{-1}$ (ΔT = 175 K). It also needs to mention that the trend of macroscopic thermal expansion measured by thermo-dilatometer is similar to that of intrinsic unit cell volume determined from the SXRD data.

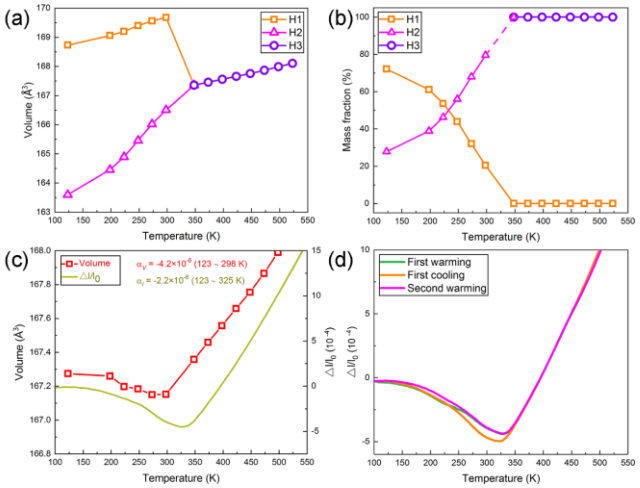

Figure 3. Temperature dependence of (a) unit cell volumes, and (b) mass fractions of H1, H2 and H3 phases. (c) The average unit cell volume as a function of temperature and liner thermal expansion ($\Delta l/l_0$) measured by a thermo-dilatometer. (d) Cyclic measurements of $Hf_{0.6}Ti_{0.4}Fe_2$ by a thermo-dilatometer.

In order to verify the reversibility of the NTE phenomenon caused by phase coexistence, macroscopic linear thermal expansion was measured for three times on the same sample. The procedure of the first heating (the green line), the first cooling (the orange line) and the second heating (the pink line) was carried out continuously (Figure 3d). Almost no thermal hysteresis can be detected for the various measurements, which provides a reliable guarantee for practical applications. In addition, the thermal expansion of other $(Hf_{1-x}Ti_x)Fe_2$ compositions (x = 0, 0.2, 0.3, 0.5, 0.6 and 1) was measured by a thermo-dilatometer (Figure S2). The widest NTE temperature range was obtained at x = 0.4 (120 ~ 325 K, ΔT = 205 K). Therefore, the composition of $(Hf_{0.6}Ti_{0.4})Fe_2$ was

selected as a representative composition to get a better comprehension on the NTE performance of $(Hf_{1-x}Ti_x)Fe_2$.

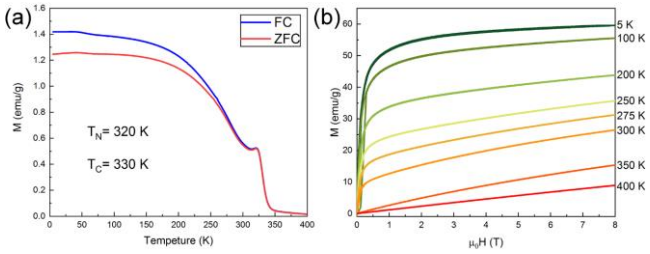

Figure 4. (a) Temperature dependences of zero-field-cooling (ZFC) and field-cooling (FC) magnetization at magnetic field of 50 Oe, and (b) magnetization curves as function of temperature and magnetic field for $Hf_{0.6}Ti_{0.4}Fe_2$.

It has been known that $Hf_{0.6}Ti_{0.4}Fe_2$ contains two phases belonging to the same space group between 120 K and 295 K. However, the reason for the phase separation is not clear. To shed light on this phenomenon, the zero-field-cooling (ZFC) and field-cooling (FC) magnetization upon heating under an applied magnetic field of 50 Oe were measured (Figure 4a). With increasing temperature, the FC-ZFC curves show a small peak at $T_N \approx 320$ K which can be regarded as a signal of magnetic phase transition from AFM to paramagnetic (PM). Subsequently, a sharp decline of magnetization is observed at $T_C \approx 330$ K, which is attributed to the transition of the FM-to-PM state. Furthermore, the isothermal magnetization curves of $Hf_{0.6}Ti_{0.4}Fe_2$ were measured at various temperatures to confirm the magnetic states at different temperatures. As shown in Figure 4b, the magnetization curve of 5 K is not saturated slightly at high fields, which indicates that small amount of nonferromagnetic components exist. These nonferromagnetic components can be inferred to be AFM, which would be proved later by NPD. When temperature rises to 350 K, the isothermal magnetization curves exhibit the PM characteristic. Based on the information both from the FC–ZFC curves and the isothermal magnetization ones, $Hf_{0.6}Ti_{0.4}Fe_2$ has a FM structure with slight AFM ingredient at low temperature. With increasing temperature, the FM structure gradually transforms into the AFM one. Nevertheless, the FM does not completely change into AFM but keeps part of it, which can be corroborated from the FC-ZFC curves. Eventually, the FM and AFM all transform into PM at a close temperature ($T_N \approx 320$ K, $T_C \approx 330$ K). Combining the results of magnetic measurements and refinements of SXRD, the temperature range of coexistence of FM and AFM structures (120 ~ 320 K) is similar to the range of phase coexistence (120 ~ 295 K). Additionally, the temperature dependence of mass fractions of H1 and H2 phases has a good correlation with the evolution of FM and AFM structures. Now, we can confirm that the AFM structure is growing in FM matrix with increasing temperature, and the large unit cell volume H1 phase has FM structure and the small unit cell volume H2 phase possesses AFM structure. In conclusion, it is the different unit cell volume between FM and AFM structures that results in the phase separation.

The NPD data of $(Hf_{0.6}Ti_{0.4})Fe_2$ refined by FULLPROF are used to illustrate the magnetic structures at 295 K (Figure S3). Form the result of the refinements, two phases with the same space group were obtained, which have different lattice parameters and corresponding to two magnetic structures. One of the magnetic structure is FM with the moment of Fe at 2a and 6h sites, which are in the ab plane and parallel to the a(b)-axis. The other phase is AFM with the moment of Fe at 6h site formed the 120° structure in the ab plane and no ordered moment at 2a site. The magnetic structure of $(Hf,Ti)Fe_2$ is similar to the results obtained by B. Li.[31] The mass fractions of FM and AFM structures at 295 K, extracted from the refinements of the NPD data, are 17.71% and 82.29%, respectively. Meanwhile, 20.47% and 79.53% corresponding to the mass fraction of H1 and H2 phases were gotten by the refinements of the SXRD patterns. The results obtained from the NPD and SXRD patterns are well consistent, which reveals the nature of NTE in the present $(Hf,Ti)Fe_2$ intermetallic compound.

In summary, an intriguing NTE has been found in $(Hf,Ti)Fe_2$ intermetallic compounds. The coexistence of two hexagonal phases occurs in the whole NTE temperature range in $(Hf_{0.6}Ti_{0.4})Fe_2$, and they exhibit FM and AFM, respectively. The FM structure have a larger unit cell volume than the AFM structure. With the increase of temperature, the FM structure transforms to the AFM ones. In this process, the total unit cell volume decreases, although both of the two phases expand with increasing temperature. This is an unusual phenomenon that the coexistence of different magnetic phases leads to a wide temperature range NTE in intermetallic compounds.

ASSOCIATED CONTENT

Supporting Information. The Supporting Information is available free of charge on the ACS Publications website. Experimental details and Supporting Figure.

AUTHOR INFORMATION

Corresponding Author

*E-mail: junchen@ustb.edu.cn.

Notes. The authors declare no competing financial interests.

ACKNOWLEDGMENT

This work was supported by the National Natural Science Foundation of China (grant nos. 21825102, 21731001 and 21590793), and the Fundamental Research Funds for the Central Universities, China (FRF-TP-17-001B). This research used resources of the Advanced Photon Source, a U.S. Department of Energy (DOE) Office of Science User Facility operated for the DOE Office of Science by Argonne National Laboratory under Contract No. DE-AC02-06CH11357.

REFERENCES

(1) Mary T A, Evans J S O, Vogt T, et al. Negative thermal expansion from 0.3 to 1050 Kelvin in ZrW2O8[J]. *Science* 1996, 272(5258): 90-92.
(2) Long Y W, Hayashi N, Saito T, et al. Temperature-induced A–B intersite charge transfer in an A-site-ordered LaCu3Fe4O12 perovskite[J]. *Nature* **2009**, 458(7234): 60.
(3) Zhang N, Li L, Wu M, et al. Negative thermal expansion and electrical properties of α-Cu2V2O7[J]. *J. Eur. Ceram. Soc.* **2016**, 36(11): 2761-2766.

(4) van Schilfgaarde M, Abrikosov I A, Johansson B. Origin of the Invar effect in iron–nickel alloys[J]. *Nature* **1999**, 400(6739): 46.
(5) Song Y, Chen J, Liu X, et al. Zero Thermal Expansion in Magnetic and Metallic Tb(Co,Fe)2 Intermetallic Compounds[J]. *J. Am. Chem. Soc.* **2018**, 140(2): 602-605.
(6) Li W, Huang R, Wang W, et al. Enhanced Negative Thermal Expansion in $La_{1-x}Pr_xFe_{10.7}Co_{0.8}Si_{1.5}$ Compounds by Doping the Magnetic Rare-Earth Element Praseodymium[J]. *Inorg. Chem.* **2014**, 53(11): 5869-5873.
(7) Huang R, Liu Y, Fan W, et al. Giant negative thermal expansion in NaZn13-type $La(Fe,Si,Co)_{13}$ compounds[J]. *J. Am. Chem. Soc.* **2013**, 135(31): 11469-11472.
(8) Zhao Y Y, Hu F X, Bao L F, et al. Giant negative thermal expansion in bonded MnCoGe-based compounds with Ni_2In-type hexagonal structure[J]. *J. Am. Chem. Soc.* **2015**, 137(5): 1746-1749.
(9) Li L F, Tong P, Zou Y M, et al. Good comprehensive performance of Laves phase $Hf_{1-x}Ta_xFe_2$ as negative thermal expansion materials[J]. *Acta Mater.* **2018**, 161: 258-265.
(10) Takenaka K, Ichigo M, Hamada T, et al. Magnetovolume effects in manganese nitrides with antiperovskite structure[J]. *Sci. Technol. Adv. Mater.* **2014**, 15(1): 015009.
(11) Wang C, Chu L, Yao Q, et al. Tuning the range, magnitude, and sign of the thermal expansion in intermetallic $Mn_3(Zn,M)_xN$ (M= Ag, Ge)[J]. *Phys. Rev. B* **2012**, 85(22): 220103.
(12) Iikubo S, Kodama K, Takenaka K, et al. Local lattice distortion in the giant negative thermal expansion material $Mn_3Cu_{1-x}Ge_x$ N[J]. *Phys. Rev. Lett.* **2008**, 101(20): 205901.
(13) Attfield J P. Condensed-matter physics: A fresh twist on shrinking materials[J]. *Nature* **2011**, 480(7378): 465.
(14) Greve B K, Martin K L, Lee P L, et al. Pronounced negative thermal expansion from a simple structure: cubic ScF_3[J]. *J. Am. Chem. Soc.* **2010**, 132(44): 15496-15498.
(15) Hu L, Chen J, Fan L, et al. Zero Thermal Expansion and Ferromagnetism in Cubic $Sc_{1-x}M_xF_3$ (M = Ga, Fe) over a Wide Temperature Range[J]. *J. Am. Chem. Soc.* **2014**, 136(39): 13566-13569.
(16) Hu L, Chen J, Sanson A, et al. New insights into the negative thermal expansion: direct experimental evidence for the "Guitar-String" effect in cubic ScF3[J]. *J. Am. Chem. Soc.* **2016**, 138(27): 8320-8323.
(17) Hu L, Chen J, Xu J, et al. Atomic linkage flexibility tuned isotropic negative, zero, and positive thermal expansion in $MZrF_6$ (M= Ca, Mn, Fe, Co, Ni, and Zn)[J]. *J. Am. Chem. Soc.* **2016**, 138(44): 14530-14533.
(18) Hu L, Qin F, Sanson A, et al. Localized Symmetry Breaking for Tuning Thermal Expansion in ScF_3 Nanoscale Frameworks[J]. *J. Am. Chem. Soc.* **2018**, 140(13): 4477-4480.
(19) Chen J, Xing X, Sun C, et al. Zero thermal expansion in $PbTiO_3$-based perovskites[J]. *J. Am. Chem. Soc.* **2008**, 130(4): 1144-1145.
(20) Chen J, Nittala K, Forrester J S, et al. The role of spontaneous polarization in the negative thermal expansion of tetragonal $PbTiO_3$-based compounds[J]. *J. Am. Chem. Soc.* **2011**, 133(29): 11114-11117.
(21) Pan Z, Chen J, Jiang X, et al. Colossal Volume Contraction in Strong Polar Perovskites of $Pb(Ti,V)O_3$[J]. *J. Am. Chem. Soc.* **2017**, 139(42): 14865-14868.
(22) Goodwin A L, Kennedy B J, Kepert C J. Thermal expansion matching via framework flexibility in zinc dicyanometallates[J]. *J. Am. Chem. Soc.* **2009**, 131(18): 6334-6335.
(23) Goodwin A L, Calleja M, Conterio M J, et al. Colossal positive and negative thermal expansion in the framework material $Ag_3[Co(CN)_6]$[J]. *Science* **2008**, 319(5864): 794-797.
(24) Giddy A P, Dove M T, Pawley G S, et al. The determination of rigid-unit modes as potential soft modes for displacive phase transitions in framework crystal structures[J]. *Acta Crystallogr A* **1993**, 49(5): 697-703.
(25) Chen J, Wang F, Huang Q, et al. Effectively control negative thermal expansion of single-phase ferroelectrics of $PbTiO_3$-(Bi, La) FeO_3 over a giant range[J]. *Sci. Rep.* **2013**, 3: 2458.
(26) Chen J, Hu L, Deng J, et al. Negative thermal expansion in functional materials: controllable thermal expansion by chemical modifications[J]. *Chem. Soc. Rev.* **2015**, 44(11): 3522-3567.
(27) Li Q, Zhu H, Zheng L, et al. Local Structural Distortion Induced Uniaxial Negative Thermal Expansion in Nanosized Semimetal Bismuth[J]. *Adv. Sci.* **2016**, 3(11): 1600108.
(28) Zheng X G, Kubozono H, Yamada H, et al. Giant negative thermal expansion in magnetic nanocrystals[J]. *Nat. Nanotechnol.* **2008**, 3(12): 724.
(29) Azuma M, Chen W, Seki H, et al. Colossal negative thermal expansion in $BiNiO_3$ induced by intermetallic charge transfer[J]. *Nat. Commun.* **2011**, 2: 347.
(30) Arvanitidis J, Papagelis K, Margadonna S, et al. Temperature-induced valence transition and associated lattice collapse in samarium fulleride[J]. *Nature* **2003**, 425(6958): 599.
(31) Li B, Luo X H, Wang H, et al. Colossal negative thermal expansion induced by magnetic phase competition on frustrated lattices in Laves phase compound $(Hf,Ta)Fe_2$[J]. *Phys. Rev. B* **2016**, 93(22): 224405.
(32)Ibarra M R, Algarabel P A. Giant volume magnetostriction in the FeRh alloy[J]. *Phys. Rev. B* **1994**, 50(6): 4196.
(33) Sun Y, Wang C, Huang Q, et al. Neutron diffraction study of unusual phase separation in the antiperovskite nitride Mn_3ZnN[J]. *Inorg. Chem.* **2012**, 51(13): 7232-7236.

TOC

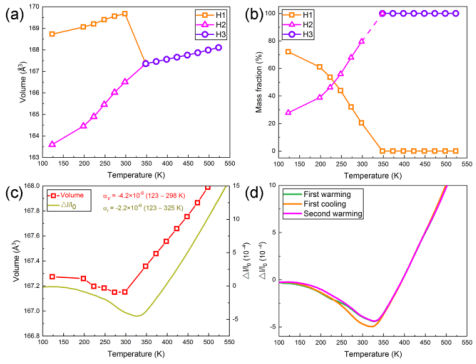

Synopsis:

Negative thermal expansion was explored in (Hf,Ti)Fe2 intermetallic compounds. The coexistence of ferromagnetic and antiferromagnetic phases with the same space group but different lattice parameter has been detected in the whole negative thermal expansion temperature range. This curious phenomenon is attributed to that unit cell volume of the antiferromagnetic phase is smaller than that of the ferromagnetic phase, and the mass fraction of antiferromagnetic phase increases with increasing temperature.